UNIVERSITY OF CALIFORNIA, SAN DIEGO

Triple Oxygen Isotope Measurement of Nitrate to Analyze Impact of Aircraft Emissions

A Thesis submitted in partial satisfaction of the

requirements for the degree Master of Science

in

Chemistry

by

Sharleen Chan

Committee in charge:

Professor Mark Thiemens, Chair
Professor Timothy Bertram
Professor William Trogler

2013

The Thesis of Sharleen Chan is approved and it is acceptable in quality and form for publication on microfilm and electronically:

_____

_____

_____
Chair

University of California, San Diego

2013

DEDICATION

To my family

whose love, inspiration, and support

made the completion of my degree possible.

TABLE OF CONTENTS

Signature Page……..……. iii

Dedication……..……..…….. iv

Table of Contents…….…….….…… v

List of Figures……..……....…. vii

List of Tables……...…….. ix

Acknowledgements……..…….……..… x

Abstract……...….....…….....…. xi

Chapter 1 Nitrate and the Nitrogen Cycle…….…….....… 1

1.1 The Nitrogen Cycle……..…….....… 1

1.2 Atmospheric nitrogen species in the Troposphere…….....…… 1

1.2.1 Leighton relationship……..…...…… 4

1.3 Consequences of anthropogenic nitrogen emissions…….….…… 4

1.4 References……...…… 6

Chapter 2 Isotopes……...……...…… 7

2.1 Isotopes of Nitrogen…… 7

2.2 Delta notation and mass-dependent isotopic fractionations…….....… 9

2.3 Mass-independent fractionations…….....…….. 12

2.4 References…….....…… 14

Chapter 3 Triple oxygen isotope measurement of nitrate to analyze impact of aircraft emissions……..…..… 15

3.1 Introduction……..……...….. 15

3.2 Experimental……...……..…… 22

3.2.1 Sample Collection……..……..…… 25

3.2.2 Nitrate Extraction and Analysis……...……...…..…… 26

3.3 Results and Discussion……..……...…… 28

3.3.1 Palmdale, CA...……...……. 28

3.3.2 Los Angeles International Airport……..... 36

3.4 Conclusions……...…… 39

3.5 Appendix…….…..…...…… 41

3.6 References……..….……..…… 45

LIST OF FIGURES

Figure 1: Diurnal variation of NO, NO_2, and O_3 showing the relationship between each species. [Finlayson-Pitts and Pitts, 2000]……...…… 3

Figure 2: Isotopic fractionation of ozone formation [Thiemens and Heidenreich, 1983]. At 0,0 ‰, the original oxygen isotopic composition exists. Molecular oxygen reservoirs are denoted by squares and the ozone product by circles. The dotted line is the mass fractionation line with slope = 0.52 passing through original isotopic composition at 0,0‰…….…… 11

Figure 3: Overview of Fischer-Tropsch process. Carbon containing feedstock is processed into Syngas (mixture of CO and H2) and undergoes the Fischer Tropsch process through catalysts into hydrocarbon chains……...…… 21

Figure 4: AAFEX campaign sampling sites located in Palmdale, CA at fixed distances from the exhaust. Distances of 1m, 30m, 145m were chosen to study the formation of particles…….…...……. 23

Figure 5: Map of the four sampling sites used in the LAX campaign. Site #1 was the closest to jet emissions situated at the east end of the south runway 25R, just behind the airfield's southeast jet blast protection screen. Site #2 was at the northwest edge of LAX closest to incoming marine air during west wind conditions. Site #3 was intended to have the direct jet emission about 1km from the airport. Site #4 was northeast of LAX and closest to freeway traffic……...……...……. 24

Figure 6: Changes in $\Delta^{17}O$ of nitrate with varying fuel types and distances (m)..... 29

Figure 7. Oxygen triple isotope plot showing the relationship between atmospheric oxygen and ozone with nitrate aerosol measurements from Palmdale, LAX, La Jolla and Coastal Antarctica……..……. 30

Figure 8: Varying fuel types showing changes in $\Delta^{17}O$ with respect to $\delta^{18}O$…….. 31

Figure 9: Seasonal representation of $\delta^{18}O$ and $\Delta^{17}O$ collected from LAX…….. 37

LIST OF TABLES

Table 1: Average comparison of properties from various fuel types and their mixtures. FT fuels contain minor amounts of sulfur and aromatic hydrocarbons, as conveyed through the higher hydrogen content and H/C ratio, compared to JP-8…...…… 20

Table 2: Palmdale Isotopic Measurements…….…….. 41

Table 3: LAX Fall 2009 Isotopic Measurements…….. 42

Table 4: LAX Winter 2010 Isotopic Measurements……...…….. 43

Table 5: LAX Spring 2010 Isotopic Measurements……...…….. 44

ACKNOWLEDGEMENTS

I would like to acknowledge many individuals whose help and support have made this work possible. First, I would like to express my deepest gratitude to my thesis advisor, Professor Mark Thiemens, for his guidance, inspiration, patience and providing me with an excellent atmosphere for conducting research. I would also like to thank Dr. Robina Shaheen for her invaluable mentorship at the conclusion of my undergraduate career and throughout my graduate career. Teresa Jackson and Dr. Subrata Chakraborty for their input in experimental design, assistance in sample processing, and for collecting all aerosols used in this thesis. Also, many thanks also to members of my lab for their helpful discussions and words of wisdom. They are: Analisa Hill, Zhi-sheng Zhang (Sun Yat-Sen University- China), Jason Hill-Falkenthal, Morgan Nunn, and Dr. Antra Priyadarshi. Special thanks to Professor Bertram and Professor Trogler for participating in my thesis defense committee. Lastly, I would also like to thank my parents, my elder brother, and my friends for supporting and encouraging all my ambitions.

Chapter 3, in part is currently being prepared for submission for publication of the material. R. Shaheen, A. Hill, T. Jackson, S. Chakraborty, The thesis author was the primary investigator and author of this material.

ABSTRACT OF THE THESIS

Triple Oxygen Isotope Measurement of Nitrate to Analyze Impact of Aircraft Emissions

by

Sharleen Chan

Master of Science in Chemistry

University of California, San Diego, 2013

Professor Mark Thiemens, Chair

With 4.9% of total anthropogenic radiative forcing attributed to aircraft emissions, jet engines combust copious amounts of fuel producing gases including: NOx (NO + NO_2), SOx, VOC's and fine particles [IPCC (1999), IPCC (2007), Lee et al., 2009]. The tropospheric non-linear relationships between NOx, OH and O_3 contribute uncertainties in the ozone budget amplified by poor understanding of the NO_x cycle. In a polluted urban environment, interaction of gases and particles produce various new compounds that are difficult to measure with analytical tools available today [Thiemens, 2006].

Using oxygen triple isotopic measurement of NO_3 to investigate gas to particle formation and chemical transformation in the ambient atmosphere, this study presents

data obtained from aerosols sampled at NASA's Dryden Aircraft Operations Facility (DAOF) in Palmdale, CA during January and February, 2009 and Los Angeles International Airport (LAX) during Fall 2009, Winter 2010, and Spring 2010. The aerosols collected from jet aircraft exhaust in Palmdale exhibit an oxygen isotope anomaly ($\Delta^{17}O = \delta^{17}O - 0.52\ \delta^{18}O$) increase with photochemical age of particles (-0.22 to 26.41‰) while NO_3 concentration decreases from 53.76 - 5.35ppm with a radial distance from the jet dependency. Bulk aerosol samples from LAX exhibit seasonal variation with $\Delta^{17}O$ and NO_3 concentration peaking in winter suggesting multiple sources and increased fossil fuel burning. Using oxygen triple isotopes of NO_3, we are able to distinguish primary and secondary nitrate by aircraft emissions allowing new insight into a portion of the global nitrogen cycle. This represents a new and potentially important means to uniquely identify aircraft emissions on the basis of the unique isotopic composition of jet aircraft emissions.

References:

IPCC, 1999 - J.E.Penner, D.H.Lister, D.J.Griggs, D.J.Dokken, M.McFarland (Eds.) Prepared in collaboration with the Scientific Assessment Panel to the Montreal Protocol on Substances that Deplete the Ozone Layer. Cambridge University Press, UK. pp 373

IPCC, 2007: Climate Change 2007: The Physical Science Basis. Contribution of Working Group I to the Fourth Assessment Report of the Intergovernmental Panel on Climate Change [Solomon, S., D. Qin, M. Manning, Z. Chen, M. Marquis, K.B. Averyt, M.Tignor and H.L. Miller (eds.)]. Cambridge University Press, Cambridge, United Kingdom and New York, NY, USA.

Lee, D.S., Fahey, D.W., Forster, P.N., Newton, P.J., Wit, R., Lim, L.L., Owen, B., Sausen, R. Aviation and global climate change in the 21st century, Atmospheric Environment (2009),doi:10.1016/j.atmosenv.2009.04.024

Thiemens, M.H. 2006, History and Applications of Mass-Independent Isotope Effects. *Annu. Rev. Earth Plnet. Sci.* 34, 217-262.

Chapter 1

Nitrate and the Nitrogen Cycle

1.1 The Nitrogen Cycle

Nitrogen is essential for the development of agricultural crops. When nitrogen is insufficient, plant growth and root systems become underdeveloped while older leaves turn yellow and the crop lacks in protein. However, too much nitrogen can delay ripeness causing excessive vegetative growth at the expense of grain yield. The delicate balance of nitrogen content needs to be maintained.

Primary pollutants known as NOx are emitted directly into the air. Secondary pollutants are formed when primary pollutants react or combine (ie. O_3). NOx is produced in high temperatures and pressures. The natural sources of NOx include: bacterial processes (ie. Nitrification oxidizes ammonia to NO_2 or NO_3), lightning (oxidizes atmospheric N_2 to NOx), and biomass burning (oxidizing organic nitrogen). Biomass burning emits different quantities of NOx as different biomass types are burned each time (tropical rain forests, savannah, boreal forests). Anthropogenic sources of NOx include: energy production in power plants, road transportation, and industrial combustion. The main sources of NOx in the troposphere include: fossil fuel combustion, fires, microbial soil emissions, lightning, oxidation of biogenic NH3, aircraft, and the stratosphere [Delmas et al., 1997].

1.2 Atmospheric nitrogen species in the Troposphere

The nitrogen cycle plays an essential role in atmospheric chemistry. Most chemical compounds are oxidized and removed from the air or transformed into other

chemical species which come in contact with NO or NO_2. In the troposphere, N_2 can be oxidized by O_2 to NO by lightning discharges or combustion processes [Warneck, 2000]

$$O_2 + N_2 \rightarrow 2NO$$

NO is quickly oxidized by the atmosphere's primary oxidants, HOx and O_3 to form NO_2 (reaction 1). NO_2 is then photolyzed by UV/VIS light (< 420nm) to reform NO and generates O_3 (reaction 2-3) [Seinfeld and Pandis, 1998].

$$NO + O_3 / HO_2 / RO_2 \rightarrow NO_2 + O_2 / OH / RO_2 \quad (1)$$

$$NO_2 + h\nu \rightarrow NO + O(^3P) \quad (2)$$

$$O(^3P) + O_2 + M \rightarrow O_3 \quad (3)$$

Steady state concentrations of NOx and O_3 are the result of the relative rate constants of reactions 1-3. The NOx cycle follows well-known daytime and night-time reaction pathways (Figure 1). At urban centers such as Pasadena, CA, the concentration of NO rises and reaches a maximum when automobile traffic peaks followed by NO_2 concentration maxima. Oxidant levels (like O_3) are relatively low in the early morning and increase significantly around noon when NO concentration is at its minimum.

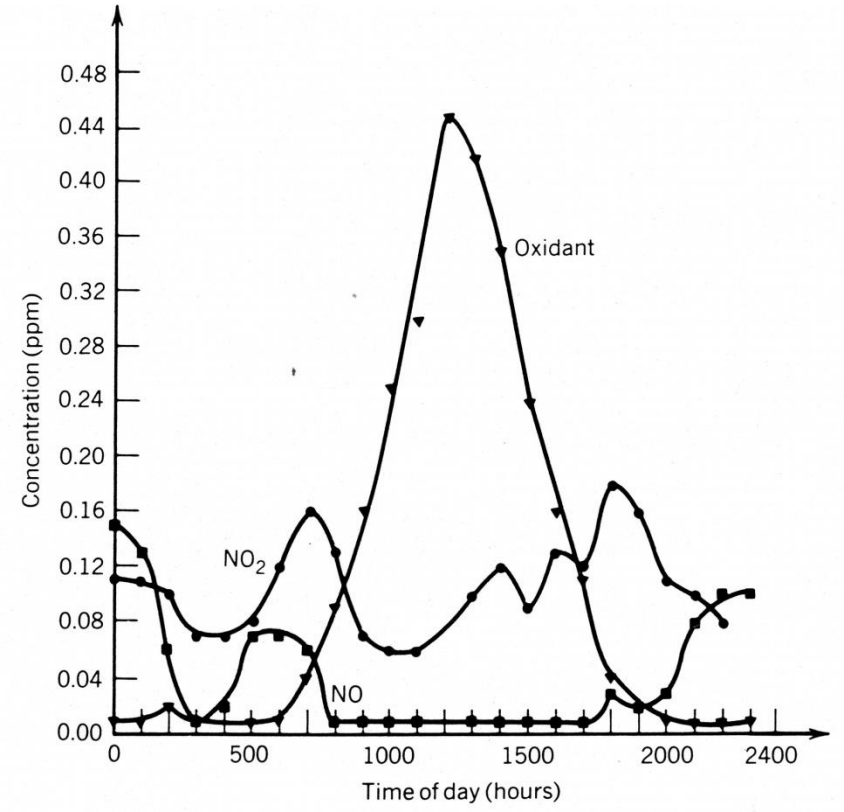

Figure 1: Diurnal variation of NO, NO_2, and O_3 showing the relationship between each species. [Finlayson-Pitts and Pitts, 2000].

During the day, highly reactive nitric acid (HNO_3) is generated by NO_2 reacting with the OH radical (reaction 4).

$$NO_2 + OH + M \rightarrow HNO_3 + M \qquad (4)$$

Additionally, NO_2 can react with O_3 to create the nitrate radical NO_3 which can form HNO_3 through hydrogen abstraction reactions involving hydrocarbons or dimethyl sulfide (DMS) in the marine boundary layer (reaction 5) [Yvon et al., 1996]. NO_3 can also react with NO_2 to form N_2O_5 which hydrolyzes on wet particles to form nitric acid (reaction 6) [Hallquist et al., 2000]. Reactions 5-6 are dominant during the night as NO_3

is rapidly photolyzed in visible light during the day (lifetime ~ $5sec^{-1}$) [Seinfeld and Pandis, 1998].

$$NO_2 + O_3 \rightarrow NO_3 + O_2;\ NO_3 + DMS / HC \rightarrow HNO_3 \qquad (5)$$

$$NO_2 + NO_3 \leftrightarrow N_2O_5;\ N_2O_5 + H_2O_{surfaces} \rightarrow 2\ HNO_3 \qquad (6)$$

Inorganic particulate nitrate ($p\text{-}NO_3^-$) and nitric acid (HNO_3) are ultimate sinks due to their high solubility and chemical stability in wet and dry depositions. Depending on season and environmental condition, the lifetime of nitrogen species varies.

1.2.1 Leighton relationship

The concentration of tropospheric ozone in areas polluted with nitrogen oxides is defined as the Leighton relationship, given by:

$$[O_3] = k_1[NO_2] / k_3[NO] \qquad (7)$$

where k_1 is the rate in which NO_2 photolyzes to NO and $O(^3P)$, and k_3 is the rate in which NO reacts with O_3 to form NO_2 and O_2. By linking the concentrations of species involved in the generation of ozone in the troposphere, the Leighton relationship exhibits how production of ozone is directly related to solar intensity. Therefore, O_3 will have the highest concentration in the day around noon and in the summer season.

1.3 Consequences of anthropogenic nitrogen emissions

Photochemical air pollution was first recognized in Los Angeles when plant pathologists observed unique damage to agricultural crops in areas of the Los Angeles basin [Middleton et al., 1950]. Since that time, photochemical air pollution is now

recognized as a world-wide problem in areas where VOCs and NOx emissions are confined by thermal inversions and irradiated by sunlight. NOx also contributes to the formation of acid rain.

In addition to driving the formation of photochemical smog and acid rain, the nitrogen cycle has other impacts including: doubling the rate of nitrogen input into the terrestrial nitrogen cycle, increasing concentrations of N_2O and other oxides of nitrogen globally, causing loss of soil nutrients, contributing to acidification of soils, streams, and lakes; and increasing transfer of nitrogen through rivers to estuaries and coastal oceans [Vitousek et al., 1997].

References:

Delmas, R., C. Jambert, and Serga. 1997. Global inventory of NOx sources. *Nutrient Cycling in Agroecosystems* 48:51-60.

Finlayson- Pitts B.J. and J.N. Pitts, 2000. Chemistry of the Upper and Lower Atmosphere, Academic Press, San Diego, CA.

Hallquist, M., Stewart, D.J., Baker,J., and Cox, R.A.. 2000. Hydrolysis of N_2O_5 on submicron sulfuric acid aerosols, J. Phys. Chem. A, 10(17), 3984-3990.

Middleton, J.T., Kendrick, J.B. Jr. and Darley, E.F..1953. Air pollution injury to crops. California Agric. 7(11): 11-12.

Seinfeld J. H. and Pandis S. N.. 1998. Atmospheric Chemistry and Physics: From Air Pollution to Climate Change, J. Wiley, New York.

Vitousek, Peter M., John D. Aber, Robert W. Howarth, Gene E. Likens, Pamela A. Matson, David W. Schindler, William H. Schlesinger, and David G. Tilman. 1997. Human alteration of the Global Nitrogen Cycle: sources and consequences. *Ecological Applications* 7:737–750.

Warneck, P., 2000. Chemistry of the Natural Atmosphere, 2nd Edition. Academic Press, Inc., New York, NY.

Yvon, S.A., J.M.C. Plan, F.R.Nien, D.J. Cooper, and E.S. Saltzman. 1996. Interaction between nitrogen and sulfur cycles in the polluted marine boundary layer, *J. Geophys. Res*., 101 (D1), 1379-1386.

Chapter 2

Isotopes

2.1 Isotopes of Nitrogen

Understanding the formation of the solar system has been pursued in some fashion or another for a significant portion of human history. The fractionation of chemical elements and its isotopes has proven essential in the study of Earth's constant cycle of its elements and isotopes. Isotopes are atoms with the same number of protons but differing number of neutrons. With the same number of protons, two isotopes are the same element and have the same number of electrons thereby having nearly identical chemical behavior.

Stable isotopes occur at natural abundance levels and is attributed to the stability of the nucleus where even-even proton-neutron nuclei are more stable than even-odd due to enhanced nuclear binding energy. The subtle mass difference distinguishes the isotopes and result in physical and chemical isotopic effects (also known as isotopic fractionation). The largest isotopic fractionation can be seen in hydrogen where the mass difference (1 or 2 atomic mass units (amu)) is proportionally largest to its total mass. Difference in mass affects the internal energy of the molecules.

Isotopes were first measured by using electric current producing ionized molecules and subsequently accelerated through a magnetic field that separates the isotopic species based on changes in angular momentum associated with their respective mass difference. The radius of the curvature for the path of different isotopic molecules is given by the following relationship:

$$r = \sqrt{\frac{2Vm}{B^2 q}}$$

where r is the radius of the charged particle q, m is the mass accelerated by voltage V through a magnetic field B. The radius of curvature is proportional to the square root of the mass to charge ratio, m/q, of the particle. This results in larger radii for the isotopic beam which provides the relative isotopic abundances when compared to a known standard ratio measured simultaneously with a dual-inlet mass spectrometer. In the case of oxygen, Standard Mean Ocean Water (SMOW) is the accepted standard containing a value of exactly 0.The measurement of isotope ratios of a sample compared to the same ratio in a standard allows very high precision in the measurement of the ratios as compared to the absolute measurement.

In the gas phase, diatomic molecules in the electronic ground state possess internal energy equal to the sum of separate contributions from electronic, vibrational, and rotational energy. Since rotational is much smaller than vibrational and electronic energies, we only consider the effect of vibration in the electronic state as the source of conventional isotope effects. At normal temperatures and pressures, almost all molecules are in their ground vibrational and electronic state. The lowest vibrational level ($\nu=0$) is raised above the energy minimum in an energy potential well by zero-point energy. As vibrational levels increase, the differences in energy between each level decreases and the interatomic distance increases. While the vibrational excitation increases, the difference in energy continues to decrease until the levels converge at the theoretical limit ($\nu=\infty$) where the complete separation of atoms occurs. If there are two isotopically substituted diatomic molecules, both species have the same electronic ground state but different

zero-point energies. Although the difference between the species is small, the physical chemical effects from the isotopes are mainly caused by this zero-point energy difference. Therefore the reaction rates and equilibrium constants slightly differ for isotopically substituted molecules involved in chemical reactions.

2.2 Delta notation and mass-dependent isotopic fractionations

Isotopic ratios are reported in δ (delta) notation which compares the relative ratios of the minor to major isotopes in a sample, R_{sample} and a standard, R_{std}. Using a example of oxygen:

$$R_{sample} = \frac{18_{O_{sample}}}{^{16}O_{sample}}$$

$$R_{std} = \frac{18_{O_{std}}}{^{16}O_{std}}$$

The expressions above are then defined in relative terms to provide the δ18O of a sample, again using the example of oxygen:

$$\delta^{18}O\ (‰) = \left[\frac{R_{sample}}{R_{std}} - 1\right] * 1000$$

The resulting δ ratio is used for expressing compositional changes and is expressed in parts per thousand (permil ‰). In a three isotope system (like oxygen), mass differences will dictate the relative rates of the isotopic species undergoing physical and chemical processes. The separation of isotopes in elements and molecules between two parts of a dynamic system is described by the fractionation factor α where:

$$\alpha_{A\text{-}B} = R_A / R_B$$

where A and B refer most simply to products and reactants of a reaction. Therefore the fractionation factor is equivalent to the rate constant for isotopes in a system. The

fractionation that occurs as a result of the removal of isotopic species from a reservoir is dictated by Raleigh distillation:

$$R/R_i = f^{\alpha-1}$$

where α is the fractionation factor, f is the fractional loss in the system, and R/Ri represents the respective ratio of the final to initial isotopic composition.

Isotopic fractionation can also be mass dependent or mass independent. Mass dependent isotopic fractionation is linearly dependent on mass and is dominant in most terrestrial solid samples. The mass dependent isotopic effect is defined from isotope with two mass units different from a reference isotope showing twice the effect of one that possess one mass unit different. In a three-isotope diagram of $\delta^{18}O$ vs. $\delta^{17}O$ (Figure 2), compositions of nearly all terrestrial samples produces a line of slope about one half (except for hydrogen isotopes) called the terrestrial fractionation line (TFL). This line reflects mass-dependent fractionation from a single homogeneous source during chemical and physical processes resulting from mass differences of oxygen isotopes. The slope (0.52) results from changes in $^{17}O/^{16}O$ that are nearly half of those in $^{18}O/^{16}O$ due to isotopic mass differences. The precise value of the slope is dependent on the nature of the isotopic species [Thiemens, 2006].

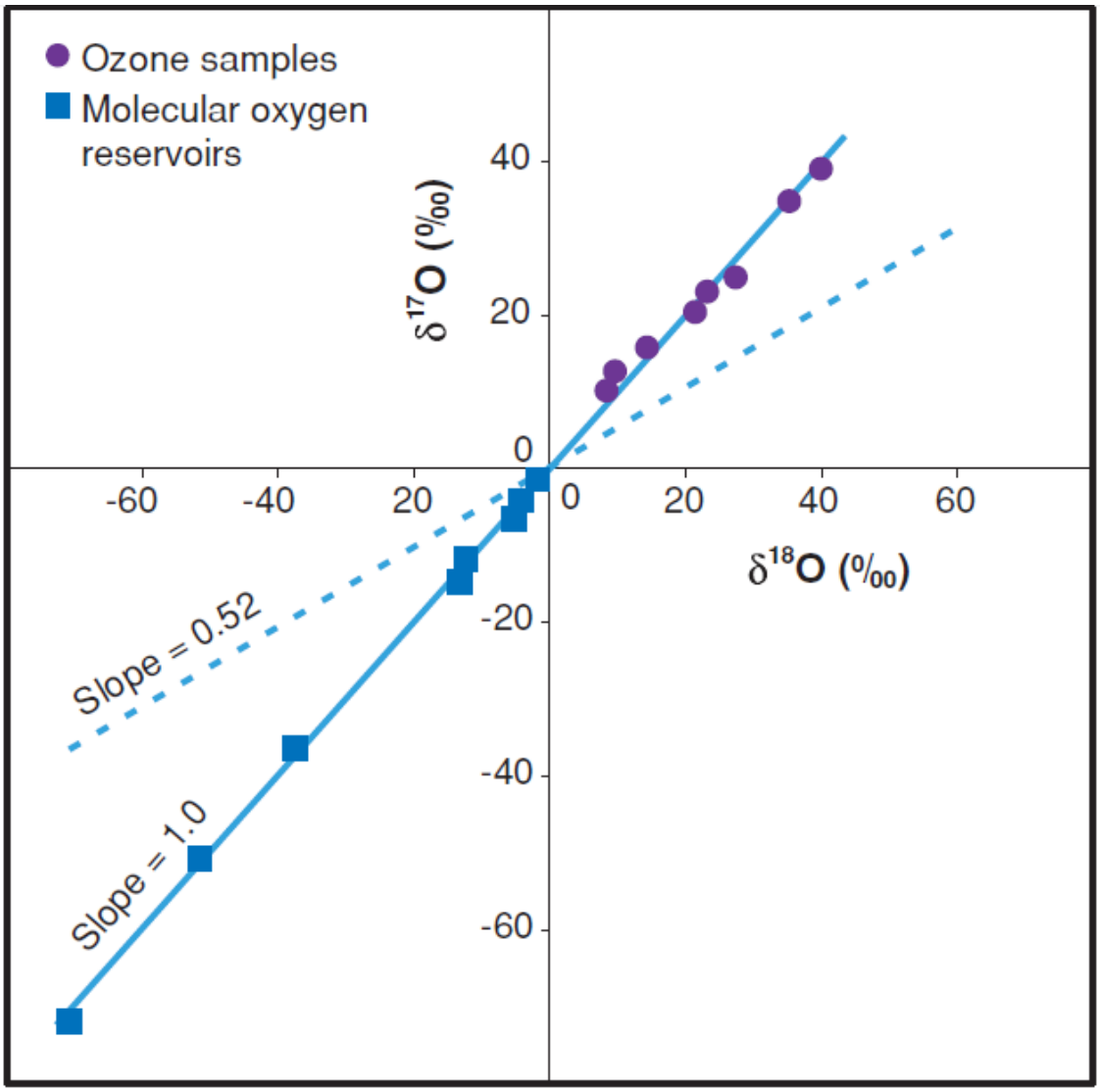

Figure 2: Isotopic fractionation of ozone formation [Thiemens and Heidenreich, 1983]. At 0,0 ‰, the original oxygen isotopic composition exists. Molecular oxygen reservoirs are denoted by squares and the ozone product by circles. The dotted line is the mass fractionation line with slope = 0.52 passing through original isotopic composition at 0,0‰.

The oxygen isotopic composition of terrestrial samples of waters and rocks is an example of mass dependent oxygen isotopic fractionation. Measurements of oxygen isotopic ratios indicate the mean ratio is 0.52 based on calculations from Rayleigh processes for oxygen-containing species of different masses and for reaction equilibria between similar species at various temperatures [Matsuhisa et al, 1978.] The natural abundance for ^{16}O, ^{17}O, and ^{18}O is 99.762%, 0.039% and 0.205%, respectively [Miller et al., 2002]. Due to the low isotopic abundances, for convenience of expressing small changes of the isotopic fractionation, isotopic compositions are normalized to Standard Mean Ocean Water (SMOW).

2.3Mass-independent fractionations

While many reactions are consistent with mass-dependent fractionation, there are also elements with small isotopic variations known as isotopic anomalies. These elements have three or more isotopes with isotopic variations which "fall off" the terrestrial mixing line (0.5) in a three isotope plot (Figure 2). This type of isotopic fractionation is known as mass independent isotopic fractionation.

Mass independent oxygen isotopic fractionation was first chemically produced in the formation of ozone from an oxygen electric discharge [Thiemens and Heidenrich, 1983]. Thiemens and Heidenrich (1983) demonstrated that the production of ozone via electrical discharge produced a mass independent relationship with nearly equal enrichment in ^{17}O and ^{18}O that can be described as $\delta^{17}O = \delta^{18}O$. Later studies also showed UV ozone production leads to the same effect [Thiemens and Jackson 1987]. The mechanism creating this anomalous isotope distribution remains to be fully described.

Heidenrich and Thiemens [1986] first postulated that the higher density of vibrational energy levels in the asymmetrically substituted molecules ($^{18}O^{16}O^{16}O$ and $^{17}O^{16}O^{16}O$ vs $^{16}O^{16}O^{16}O$) will yield differential stabilization probabilities for these isotopomeric symmetric vs asymmetric species. The asymmetric species has a higher density of empty states leading to a longer lifetime in the transition state thereby making it a more stable intermediate. The studies on this mass independent isotopic effect are directly related to the understanding the ozone isotopic fractionation in the atmosphere and chemical kinetics, and its primary implication in meteoritic studies.

Measurements of mass independent fractionation effects have proven to be a strong tool in understanding chemical oxidation processes. The short-lived character of ozone and other atmospheric oxidant species are difficult to observe in concentration, but isotopic ratios provide unique tools for observing various physical and chemical processes in biogeochemical cycles, especially those associated with radical chemistry.

References:

Heidenreich J.E. III and Thiemens M.H. 1986. A non-mass-dependent oxygen isotope effect in the production of ozone from molecular oxygen: the role of symmetry in isotope chemistry. *J. Chem. Phys*. 84: 2129-36.

Matsuhisa Y., Goldsmith J. R. and Clayton R. N. 1978. Mechanisms of hydrothermal crystallization of quartz at 250°C and 15 kbar. *Geochim. Cosmochim. Acta* 42, 173-182

Miller, M. 2002. Isotopic fractionation and the quantification of 17-O anomalies in the oxygen three-isotope system: an appraisal and geochemical significance. *Geochim. Cosmochim. Acta* 66:1881-89.

Thiemens, M.H., and Heidenreich J.E. III. 1983. The mass-independent fractionation of oxygen: a novel isotope effect and its possible cosmochemical implications. *Science* 219: 1073-75.

Thiemens, M.H. and Jackson, T. 1987. Production of isotopically heavy ozone by ultraviolet light photolysis of O2. *Geophys. Res. Lett.* 14:624-27.

Thiemens, M. H. 2006. History and Applications of Mass-Independent Isotope Effects. *Annu. Rev. Earth Planet. Sci.* 34, 217-262.

Chapter 3

Triple oxygen isotope measurement of nitrate to analyze impact of aircraft emissions

Introduction:

Anthropogenic influence on atmospheric chemistry is generally assumed to coincide with the start of the Industrial Revolution – mostly due to increased emissions from fossil fuel burning [Finlayson-Pitts and Pitts, 2000]. As global economies recover, the Federal Aviation Administration (FAA) predicts air travel to nearly double in the next 20 years from 731 million passengers in 2011 to 1.2 billion passengers in 2032. [FAA aerospace Forecast Fiscal Years 2012-2032]. The increase in passenger traffic correlates with new aircraft model development, more efficient and cost effective fuels, and more flights. In 2012, 36,017 million gallons of fuel was consumed by U.S. civil aviation aircrafts [FAA Aerospace forecasts]. Approximately 9% of fuel used in the U.S. by mobile sources is jet aircraft fuel. [Sawyer et al., 2000] In California, that percentage is higher with 17% of mobile fuel in California categorized as jet fuel. As a kerosene grade distillate fuel, jet fuel contains very low sulfur content and does not generate significant SO_2 emissions. However, jet engines emit high concentrations of NOx, especially during take-off with emissions ranging from 30 to 45g NOx per kg of fuel (10-20x that of an automobile) [Baughcum, 1996]. Normal emissions at cruising altitude are a factor of 10 lower and the emissions of NOx in North America from jet aircraft are estimated to be less than 1% of the total NOx emissions [Sawyer et al., 2000].

Studies examining ground-based, on-wing engine emissions tests have been conducted including: Atmospheric Effects of Aviation Project (AEAP), Ultra-Efficient

Engine Technology (UEET) and Fundamental Aeronautics Program (FAP). These successful campaigns investigated different aspects of the impact aircrafts and their fuels have on the atmosphere. AEAP assessed chemical and climate impacts of aircraft emissions while UEET characterized engine/ combustor emissions focusing on the interaction of particles. FAP was the first evaluation of alternative fuels and new combustor technology while developing and validating tools for predicting emissions. These NASA studies have led to the confirmation of role which fuel sulfur plays in forming volatile exhaust particles, proving that ground tests yield data representative of in-flight emissions, and examine contrails and aviation impacts on upper troposphere and lower stratosphere chemistry.

Oxygen isotopes of nitrate contain the non-mass dependent relationship between oxygen-17O ($\delta^{17}O$) and oxygen-18 ($\delta^{18}O$) which is defined by $\Delta^{17}O\text{-}NO_3$ [Michalski et al., 2003; Savarino et al., 2007; Morin et al., 2008; McCabe et al., 2007]. Typical mass-dependent fractionation processes have the relationship of $\delta^{17}O \approx 0.5 \times \delta^{18}O$ whereas mass independent fractionation (MIF) deviates from this relationship and is defined by the linear approximation $\Delta^{17}O = \delta^{17}O - 0.52\ \delta^{18}O$ where $\Delta^{17}O=0$ is mass dependent. Non zero $\Delta^{17}O\text{-}NO_3$ is derived from the oxygen atom transfer from the mass-independent composition of ozone during NO_x (NO,NO_2) oxidation. Laboratory experiments show ozone production leads to a mass independent fractionation (MIF) of oxygen isotopes, $\delta^{17}O$ and $\delta^{18}O$ [Thiemens and Heidenreich, 1983]. Measurements of $\Delta^{17}O\text{-}\ NO_3$ = 20-30‰ have been measured in urban atmospheres and have generated information concerning the N cycle and oxidative capacity of the atmosphere. [Michalski et al., 2004;

Michalski et al., 2005] The measurement of triple oxygen isotope ratios in nitrate has been utilized to identify the different sources of nitrate and the partitioning between gas phase and aqueous phase oxidation pathways of NO_3 in the atmosphere [Michalski et al., 2003; Savarino et al., 2007; Morin et al., 2008; McCabe et al., 2007].

The non-linear relationships between NOx, OH, and O_3 in the troposphere influence $\Delta^{17}O$ in nitrate uniquely due to varying chemical transformation processes. In the troposphere, NO is quickly oxidized by the atmosphere's primary oxidants, HOx and O_3 to form NO_2 (reaction 1). NO_2 is then photolyzed by UV/VIS light (< 420nm) to reform NO and generate O_3 (reaction 2-3) [Seinfeld and Pandis 1998].

$$NO + O_3 / HO_2 / RO_2 \rightarrow NO_2 + O_2 / OH / RO_2 \quad (1)$$

$$NO_2 + h\nu \rightarrow NO + O(^3P) \quad (2)$$

$$O(^3P) + O_2 + M \rightarrow O_3 \quad (3)$$

Steady state concentrations of NOx and O_3 are the result of relative rate constants of reactions 1-3. The NOx cycle follows well-known daytime and night-time reaction pathways. During the day, highly reactive nitric acid (HNO_3) is generated by NO_2 reacting with the OH radical (reaction 4).

$$NO_2 + OH + M \rightarrow HNO_3 + M \quad (4)$$

Additionally, NO_2 can react with O_3 to create the nitrate radical NO_3 which can form HNO_3 through hydrogen abstraction reactions involving hydrocarbons or dimethyl sulfide (DMS) in the marine boundary layer (reaction 5) [Yvon et al., 1996]. NO_3 can

also react with NO_2 to form N_2O_5 which hydrolyzes on wet particles to form nitric acid (reaction 6) [Hallquist et al., 2000]. Reactions 5-6 are dominant during the night as NO_3 is rapidly photolyzed in visible light during the day (lifetime ~ $5sec^{-1}$) [Seinfeld and Pandis, 1998].

$$NO_2 + O_3 \rightarrow NO_3 + O_2;\ NO_3 + DMS / HC \rightarrow HNO_3 \qquad (5)$$

$$NO_2 + NO_3 \leftrightarrow N_2O_5;\ N_2O_5 + H_2O_{surfaces} \rightarrow 2\ HNO_3 \qquad (6)$$

Inorganic particulate nitrate ($p\text{-}NO_3^-$) and nitric acid (HNO_3) are ultimate sinks due to their high solubility and chemical stability in wet and dry depositions.

Alternative fuels in aircrafts have been widely studied due to increased interest in increasing aviation fuel sources, increasing fuel security and reducing particulate emissions. In the quest for alternatives to petroleum, hydrocarbon productions from renewable sources are ideal. This NASA-sponsored study isotopically investigates emissions from aircraft fuels made via the Fischer-Tropsch (FT) process and JP-8 as well as Auxiliary Power Unit (APU) emissions.

JP-8 is a standard, refined kerosene-type aircraft fuel used by the U.S. military as a replacement for diesel fuel. It has a variety of uses in heaters, stoves, tanks, nearly all diesel fuel in engines of ground vehicles and generators, and as a coolant in engines. The fuel was adopted by the U.S. Air Force in 1996 because it is a less flammable and hazardous fuel is better for safety, and combat survivability. Containing up to 20% aromatics by volume, JP-8 contains soot precursors including: benzene, toluene, and polymerized soot constituents.

Fischer-Tropsch (FT) fuels undergo Fischer-Tropsch synthesis (FTS) converting a mixture of CO and H_2 into liquid hydrocarbons of varying chain lengths by producing synthetic lubrication oil. FTS begins as the mixture of CO and Hydrogen (called synthetic gas or syngas) reacts with catalysts (usually transition metals like cobalt, iron, and ruthenium) at high temperatures to facilitate hydrocarbon formation. This process can transform any available carbon source into hydrocarbon chains. Although FTS does not create energy, it converts heat energy into chemical energy stored in the hydrocarbon bonds [Schultz, 1999]. An overview of the Fischer-Tropsch process is depicted in Figure 3. Dependent on carbon containing feedstock, this low-sulfur diesel fuel is a relevant substitution for aviation fuels due to the high energy density requirements of efficient flight travel and energy storage options. Once natural petroleum reserves are exhausted, synthetic fuel will likely become the only feasible aviation fuel due to its high energy density. FTS processes can also produce fuel in large scale quantities [Bisio, 1995].

The two fuels derived from FTS used in this study are FT-1 and FT-2. FT-1 was synthesized from natural gas by Shell Corporation and provided by the Air Force Research Lab (AFRL). FT-2 was prepared from coal by Sasol and supplied by the AFRL. Table 1 shows an average comparison between JP-8, FT-1, FT-2, and a combination of their blends. FT fuels contain minor amounts of sulfur and aromatic hydrocarbons, as conveyed through the higher hydrogen content and H/C ratio, compared to JP-8. Due to their lower aromatic, oldefinic, and long-chain hydrocarbon contents, FT fuels have a lower specific gravity than JP-8.

Table 1: Average comparison of properties from various fuel types and their mixtures. FT fuels contain minor amounts of sulfur and aromatic hydrocarbons, as conveyed through the higher hydrogen content and H/C ratio, compared to JP-8.

TEST	JP-8	FT1	FT1 Blend	FT2	FT2 Blend
Sulfur (ppm)	1148	19	699	22	658
Aromatics (%vol)	18.6	0	8	0.6	9.1
Distillation, deg C					
IBP	158	157	156	160	158
10%	176	162	166	167	170
20%	184	164	170	170	175
50%	207	170	183	180	190
90%	248	186	232	208	233
EP	273	206	264	231	263
Residue (%vol)	0.8	0.9	1	1	0.8
Loss (%vol)	0.8	0.9	1	0.9	0.9
Flash Point, deg C	46	41	43	42	46
API Gravity	41.9	60.2	50.5	54	47.9
Freezing Point, deg C	-50	-54	-60	<-80	-60
Viscosity, mm^2/s	4.7	2.6	3.3	3.6	4.1
Cetane Index	41	58	46	51	45
H Content (%mass)	13.6	15.5	14.5	15.1	14.3
Naphtalenes (%vol)	1.6	0	0.8	0	0.8
Heat of Combustion (MJ/kg)	43.3	44.4	43.8	44.1	43.8
Olefins (%vol)	0.9	0	0.6	3.8	3.3
Fuel H/C ratio	1.88	2.19	2.02	2.12	1.99
Specific Gravity	0.816	0.738	0.777	0.763	0.789

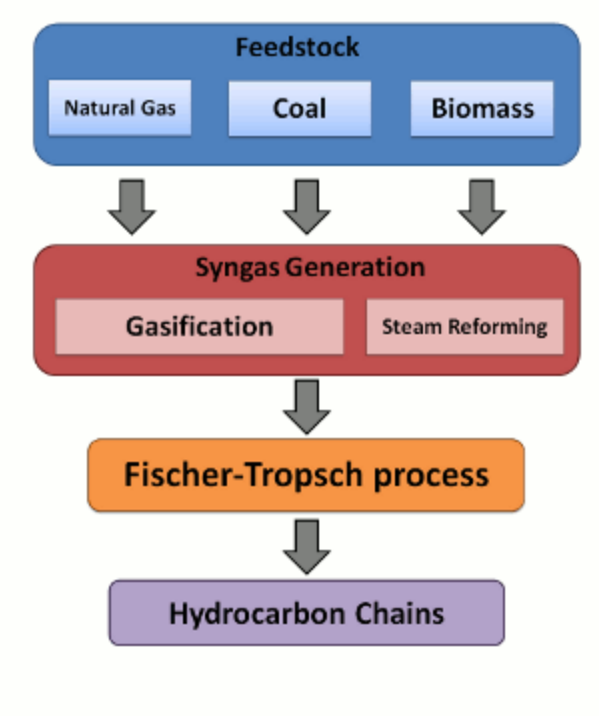

Figure 3: Overview of Fischer-Tropsch process. Carbon containing feedstock is processed into Syngas (mixture of CO and H2) and undergoes the Fischer Tropsch process through catalysts into hydrocarbon chains.

Auxiliary Power Units (APUs) are used to provide power needed for the start-up of aircraft engines. APUs typically operate when the aircraft is parked at the gate and sometimes during taxi in/ taxi out. Designed to run non-vital electrical systems when the engines are shut down, APU are primarily used to provide electricity, compressed air, air conditioning, and aircraft power when on the ground. Additionally, APUs can provide backup electric power during in-flight operations. Installed in most aircraft, APUs can alter the size and quantity of particles being emitted and be a significant source of air pollution emissions depending on the level of fuel usage [Kinsey et al., 2012]. Despite their widespread use, there is very limited information and regulation for APU usage.

In an effort to further understand plume chemistry and the origin and fate of nitrate emitted from aircrafts, we report here a study based on aerosol samples collected in Greater Los Angeles County. This study presents the first investigation of primary and secondary oxygen isotopes of nitrate emitted from aircraft and its role in the production of ozone.

Experimental:

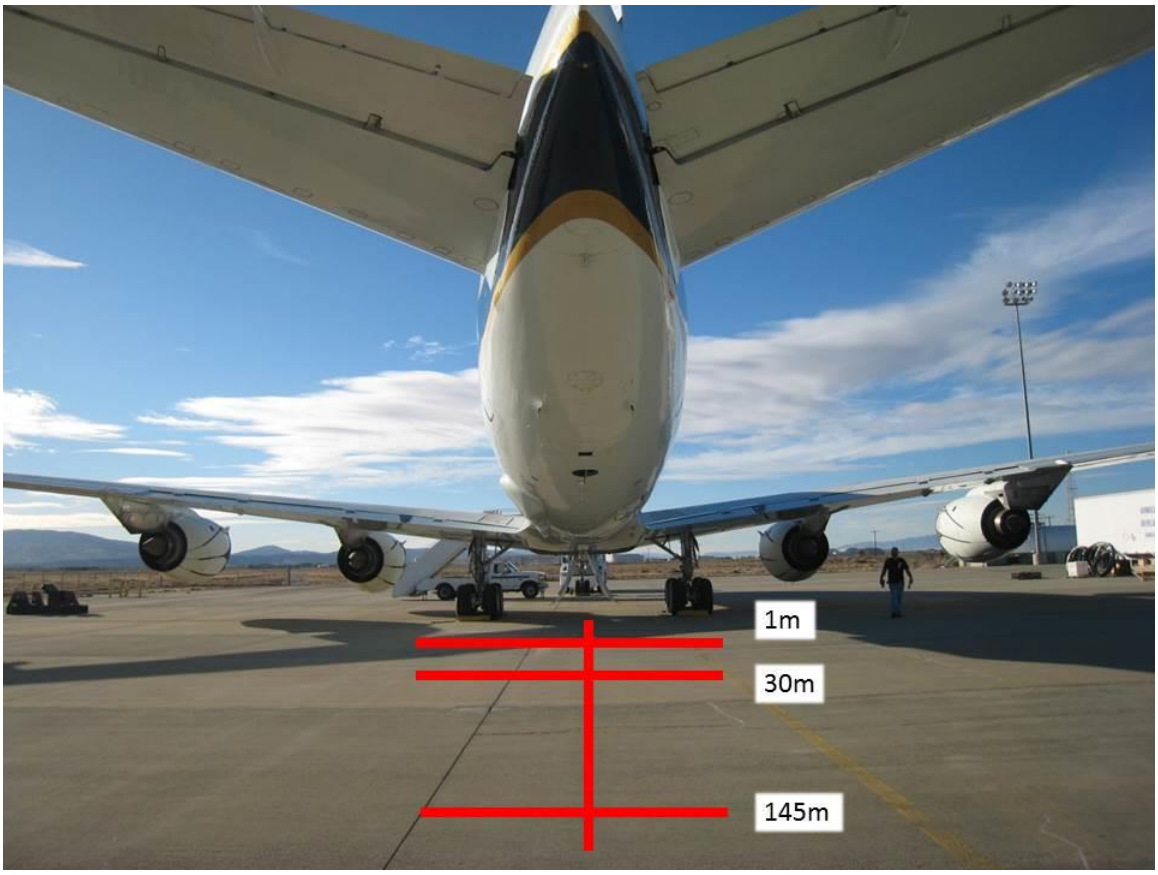

Figure 4: AAFEX campaign sampling sites located in Palmdale, CA at fixed distances from the exhaust. Distances of 1m, 30m, 145m were chosen to study the formation of particles.

Figure 5: Map of the four sampling sites used in the LAX campaign. Site #1 was the closest to jet emissions situated at the east end of the south runway 25R, just behind the airfield's southeast jet blast protection screen. Site #2 was at the northwest edge of LAX closest to incoming marine air during west wind conditions. Site #3 was intended to have the direct jet emission about 1km from the airport. Site #4 was northeast of LAX and closest to freeway traffic.

Sample Collection:

Bulk aerosol samples were collected on glass fiber filters during January and February 2009 at NASA Dryden Aircraft Operations Facility in Palmdale, CA and in 3 two-week campaigns in various seasons (fall 2009, winter 2009 and spring 2010) at Los Angeles International Airport (LAX). The sampling periods were chosen to give ample sample and damp out short time variability in their varying conditions.

At the NASA Dryden Aircraft Operations Facility in Palmdale, California, three sampling locations (Figure 4) were established using Hi-Volume cascade impactors (Hi Q Environmental, with air flow rates of 40 $feet^3$ min^{-1}). These samplers were positioned at varying distances away from the engine exhaust- 1m, 30m, and 145m to examine plume chemistry and particle evolution in time. Engine tests were performed between 5:00 and 16:00 local time with temperature ranging from -5°C at sunrise to 20°C in the mid-afternoon. However, the sampling time periods lasted averaged 4 hours and can be categorized as day or nighttime samples.

At LAX, four sampling locations were established using Hi-Volume cascade impactors (Hi Q Environmental, with air flow rates of 40 $feet^3$ min^{-1}) as seen in Figure 5. Site #1 was the closest to jet emissions situated at the east end of the south runway 25R, just behind the airfield's southeast jet blast protection screen. Site #2 was at the northwest edge of LAX closest to incoming marine air during west wind conditions. Site #3 was intended to have the direct jet emission about 1km from the airport. Site #4 was northeast of LAX and closest to freeway traffic. Each filter sample contains 4-5 days of bulk samples as both day and night particles are collected.

Nitrate Extraction and Analysis:

After collection, filters were transported back to the laboratory at UCSD, La Jolla, CA for extraction of soluble species and isotopic analysis. Filters were placed in 40mL of ultra-pure water in a centrifugal filter unit (Millipore Centricon plus-70) and sonicated for 1 hr prior to filtration into a centrifuge tube using a vacuum-operated Steriflip filter unit. An aliquot (1mL) of the filtered sample solution was diluted with 4 mL Millipore H_2O for quantification using a Dionex 2020i ion chromatograph and Dionex Ionpac A S4A anion column. Following quantification, another aliquot of sample was used to complete the isotopic analysis. 10mL of 30% H_2O_2 was added to the sample and incubated in a 70°C oven until all liquid was evaporated to remove unwanted organics. Nitrate was separated from other anions and isolated using a Dionex HPIC-AS3 high capacity anion column to convert the salts contained in the sample into HCl, HNO_3, and H_2SO_4 solutions. Nitrate salts (as KNO_3) were converted into HNO_3 using a cation exchange membrane (Dionex AMMS-4ml suppression column).

Collected HNO_3 was further converted to $AgNO_3$ by a multiple step purification scheme involving the addition of Ag_2O [Silva et.al., YEAR]. After addition of Ag_2O to HNO_3, the $AgNO_3$ solutions were freeze-dried using a Savant Speed Vac Concentrator SVC 100h and cleaned to remove excess Ag_2O. The cleaning process utilizes SPE Bulk Sorbent High Capacity C18 and cross-linked polyvinylpyrrolidone in pre-packed columns and gravity dripping small multiple increments of sample. After cleaning, the sample is freeze-dried again to remove all liquid and transferred into silver capsules (99.9% pure) using 40uL of Millipore H_2O. After drying the sample in a 70°C oven, the

silver boat is transferred onto the nitrate vacuum system and thermally decomposed into O_2 and NO_2 by heating *in vacuo* at 520°C. The vacuum system is used to avoid contamination as gases mix rapidly. NO_2 gas was separated and retained using a series of liquid nitrogen traps while O_2 was collected on molecular sieves for isotopic analysis. Finnigan-MAT 253 isotope ratio mass spectrometer was used to determine $^{18}O/^{16}O$ and $^{17}O/^{16}O$ isotopic ratios with respect to $^{16}O^{16}O$. $\Delta^{17}O$ values for the complete experimental method were determined with ± 0.2‰ precision. Complete details of the experimental method may be found in Michalski et al. [Michalski et.al., 2002]. The nitrate reference material used in this study was USGS-35 which has $\delta^{18}O$ =+25.6‰ and $\delta^{17}O$ = +57.5‰ [Bohlke et al., 2003].

Results and Discussion:

I. Palmdale, CA (34.6294°N, 118.0844°W, 775m)

Samples were collected at varying distances (1m, 30m, and 145m) from the stationary aircraft located at NASA's Dryden Aircraft Operations Facility (DAOF) in Palmdale, CA between January 19, 2009 and February 3, 2009 during the Aviation Alternative Fuels Emissions Experiment (AAFEX or AAFEX-1). AAFEX utilized National Aeronautics and Space Administration (NASA) DC-8 research aircraft testing different fuels: JP-8, natural gas derived Fischer Tropsch fuel (FT-1), and coal-derived Fischer Tropsch fuel (FT-2). Emissions from a Garrett-AiResearch (now Honeywell) Model GTCP85-98CK auxiliary power unit (APU) were also measured in this campaign.

The primary goal of the AAFEX campaign was to determine the change in gaseous and particulate emission when FT fuel is burned in comparison to regular JP-8 fuel. Fresh emissions near the exhaust plane and downwind plumes were measured to determine the effects of aging based on aerosol concentrations and isotopic composition (Figure 4).

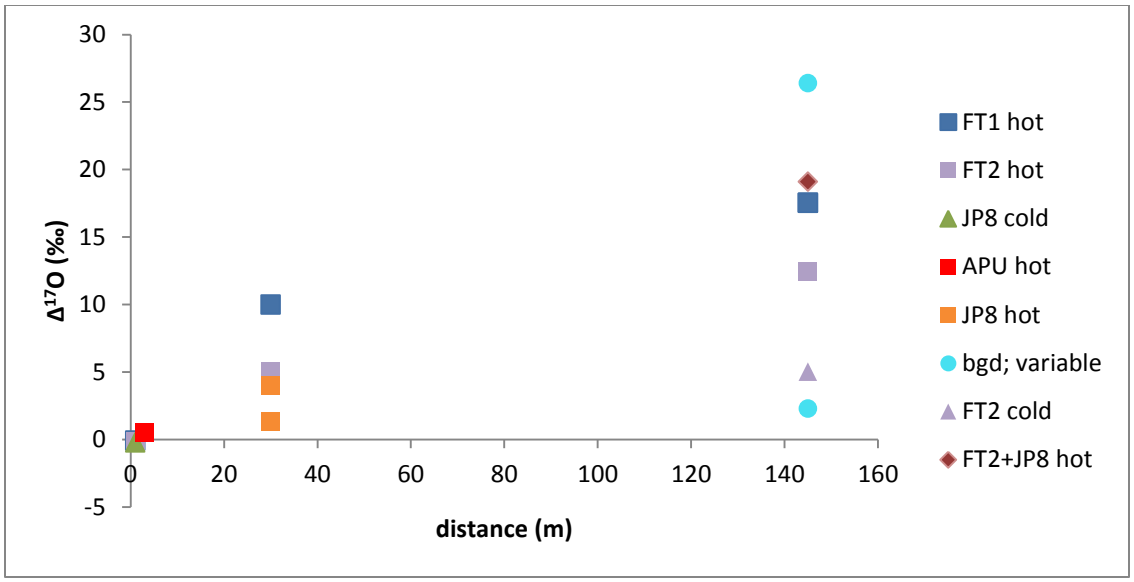

Figure 6: Changes in $\Delta^{17}O$ of nitrate with varying fuel types and distances (m).

$\Delta^{17}O$ of various fuel types collected aerosols and their isotopic composition were plotted with distance. The data reveal a direct correlation between increase in distance and in range for the $\Delta^{17}O$ values. As the distance from combustion source increases, the average $\Delta^{17}O$ at 1m, 30m, and 145m increase to values of 0.01‰, 6.36‰, and 18.60‰, respectively (Figure 6). The concentration of nitrate correspondingly decreased from 53.76ppm- 5.35ppm with increasing distance (1-145m).

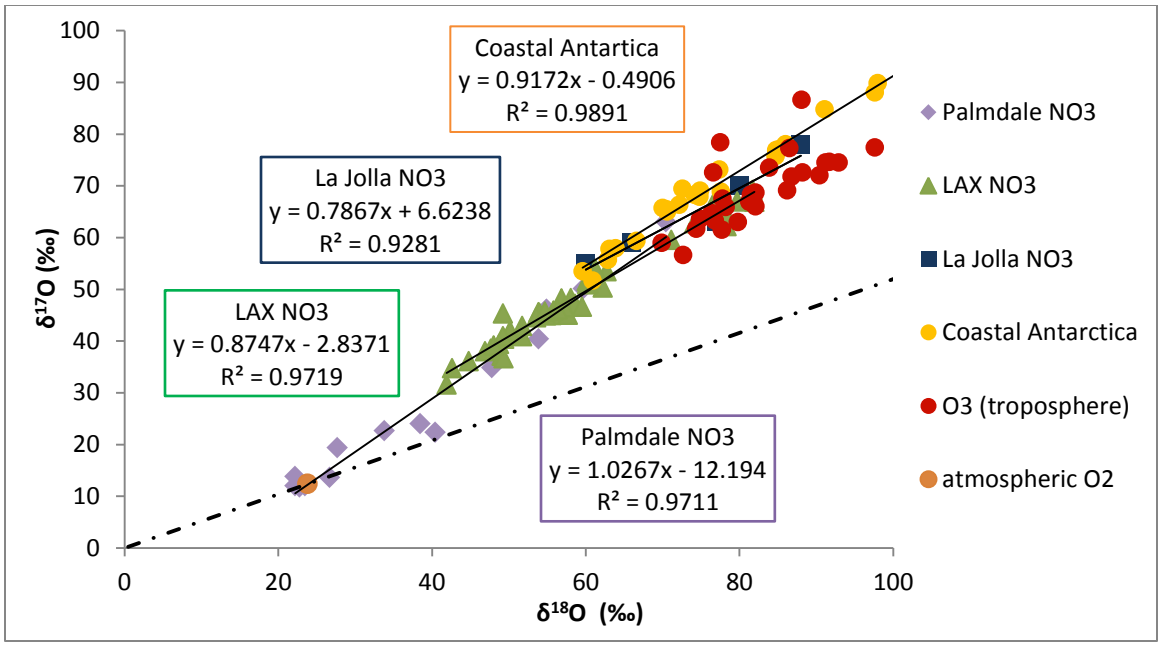

Figure 7. Oxygen triple isotope plot showing the relationship between atmospheric oxygen and ozone with nitrate aerosol measurements from Palmdale, LAX, La Jolla and Coastal Antarctica.

The $\delta^{18}O$ versus $\delta^{17}O$ plot (Figure 7) depicts nitrate isotopic data taken from the present study, as well as, from locations, including LAX, La Jolla (Michalski et al., 2003) and Coastal Antarctica (Savarino et al, 2007). All NO_3 data collected from Palmdale and LAX falls between atmospheric O_2 and O_3 isotopic values. An air sample with no photosynthetic O_2 has $\Delta^{17}O$ =0‰, $\delta^{17}O$ = 11.778‰, and $\delta^{18}O$ = 22.960‰ [Thiemens et al., 1995]. Tropospheric ozone has isotopic values ranging from: $\delta^{18}O$ =69.9 - 97.6‰, $\delta^{17}O$=56.6 - 86.6‰, and $\Delta^{17}O$=36.7 - 57.4‰ [Johnson et al., 2000].

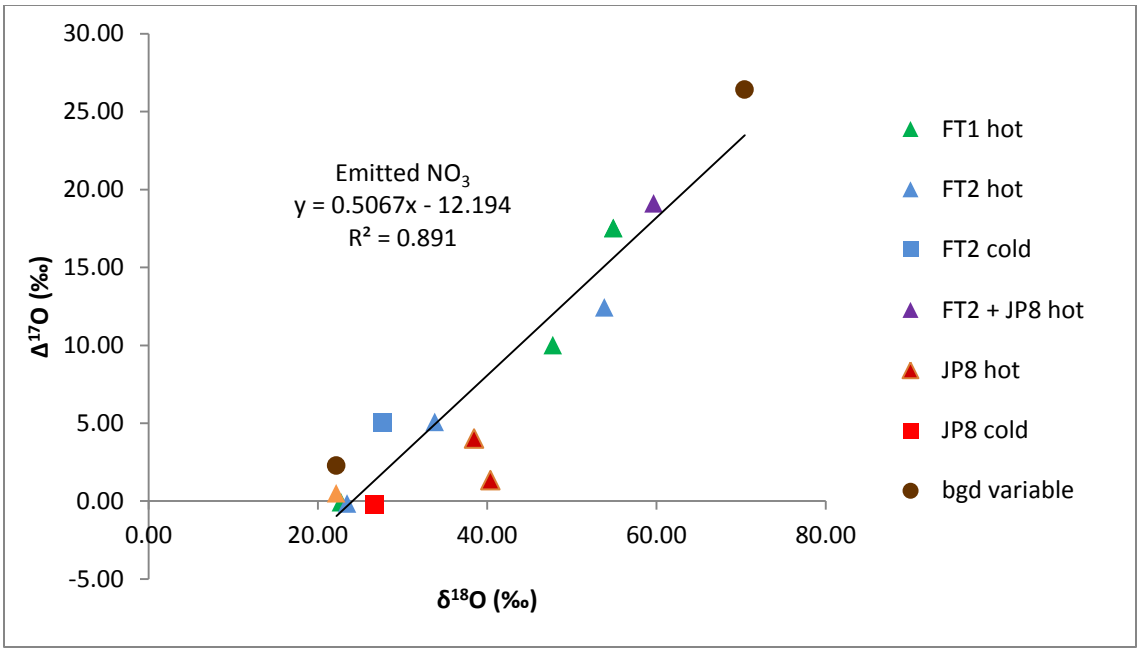

Figure 8: Varying fuel types showing changes in $\Delta^{17}O$ with respect to $\delta^{18}O$

A representation of different fuel types with varying temperature/ light reactivity is depicted in Figure 8. The square markers indicate cold temperatures (~28-50°F) and morning sampling (predawn-8am) whereas triangle markers indicate warm temperatures (~55-70°F) and midday sampling. Despite different oxidation chemistry, primary NO_3 is measured ($\Delta^{17}O$ =0) and interaction of primary NO_3 with O_3 giving rise to secondary NO_3 is depicted on the same treadline (R^2=0.891).

As primary NOx is emitted, Palmdale samples show NOx being converted into particle NO_3 as NO_3 particles sampled at 1m have isotopic values similar to atmospheric O_2 ($\Delta^{17}O$=0‰) and are less chemically evolved than NO_3 particles sampled at further distances. Through time evolution (and in this case the associated distance from the jet source, particles are diluted and cycled through oxidation reactions to eventually obtain

isotopic compositions similar to bulk nitrate values- acting as a fingerprint of ozone formation (Figure 6).

Positive $\Delta^{17}O$ of nitrate originates primarily from NOx oxidation by O_3 [Michalski et al., 2003; Lyons, 2001]. NOx rapidly achieves isotopic equilibrium with O_3 and RO_2/HO_2 as the photo-stationary state of NOx (reactions 1-3) is several orders of magnitude faster than its removal reactions (reactions 4-6). Therefore, $\Delta^{17}O$ of nitrate is a function of the relative degree of oxidation by O_3 and HO_2/RO_2. [Alexander et al., 2004]. Variation in $\Delta^{17}O$ is due to shifts of relative importance of each termination reaction with OH dominated systems (reaction 4) giving the lowest $\Delta^{17}O$ value and O_3 dominated systems (reaction 5) giving the highest $\Delta^{17}O$ value [Michalski et al., 2003]. Despite the differences in fuel types, the oxidation trend line (Figure 8) indicates the same overall reaction cycle taking place if given enough time to cycle and isotopically evolve in three isotope space. This suggests that the process of aircraft fuel combustion is the source of nitrate rather than the fuel type being burned and it is the specifics of the combined high temperature/pressure associated with jet turbines. This contributes to a previous AAFEX study which concluded greenhouse gas emissions (CO_2, CH_4, and N_2O) were not significantly influenced by fuel composition [AAFEX report].

The combustion process allows hot NO to isotopically react and isotopically exchange with ambient N_2. There is no change in $\Delta^{17}O$ from the TFL as primary NOx is emitted from the exhaust at 58 kg/min at 220°C [AAFEX report] and it is expected that the oxygen would be equilibrated with atmospheric molecular oxygen, which is mass dependent to within 0.1 per mil. As exhaust emissions are pressurized out of the aircraft

in the plume, a dispersion effect takes place as emitted NOx dilutes with ambient air. Consequently, emitted NOx cools and undergoes photolysis as distance from source increases to form NO_2 and NO_3 particles. Turbulence from the propulsion fans also contribute to increased cycling rate and generation of NO_3. Comprised primarily of soot due to high temperature combustion, the plume cools as it ages allowing for the condensation of volatile species. The observation that the samples acquired nearest the jet as being mass dependent and, equal in isotopic character to molecular oxygen is entirely consistent with this. Furthermore, there are no known sources of nitrate with this value and consequently they are highly source specific, and potentially a tracer for jet emissions.

Figure 6 indicates new nitrate particles are diluted with ambient air during the process of combustion increasing boundary layer photochemical O_3 production due to increased surface area for interactions to take place (plume emission from jet), or for secondary, lower temperature nitrate formation reactions to occur in the expanding plume. The emitted NO_x species are photolyzed in the daytime and generate $O(^3P)$ which produces ozone upon reaction with O_2 . Subsequent, well known chemical reaction networks allow interaction of NO_x with O_3 and catalytic recycling generates the oxygen isotope anomaly in the product nitrate particles may serve as a new probe for the photochemical age of air masses. As Figure 6 reveals, the isotopic source is isotopically single valued, and the secondary reactions allow evolution towards background nitrate. Unfortunately, the chemical composition of the NOx, O_3 species as well as aerosols in the relevant plume conditions for this study are not known to facilitate a chemical network

analysis of the products; future studies however can further develop a detailed chemical and isotopic analysis of the products.

During the "cold" predawn to 8am sampling periods, sink reactions for nitrate and ozone were more dominate due to the lack of sunlight to provide the photochemistry. As the day progresses, sunlight slowly allow the NOx cycle to proceed through photolysis (Figure 1). By the afternoon, temperatures rise causing gases to interact more rapidly and the "hot" midday samples are dominated by photolysis reactions to complete the full NOx cycle thereby generating O_3 (Figure 8). Without sufficient light for photolysis, the NOx cycle is not optimally operative, minimal ozone is generated, and consequently $\Delta^{17}O$ is not affected as shown in Figure 8. However, the high temperature from combustion of fuels creates a condensation effect on NO_3 and emitted soot particles formed allowing for N_2O_5 to react.

Samples collected in La Jolla and Antarctica possess elevated tropospheric nitrate isotopes compared to LAX and Palmdale aerosol samples (Figure 7). This is likely due to dominance of different chemical reactions based on the location. Antarctica samples are considered to be dominated by natural influences (stratospheric N_2O destruction, biomass burning, lightning, and/or ocean) [Wolff, 1995; Wagenbach et al., 1998] and have been suggested to be higher in concentration due to nitrate sedimentation from polar stratospheric clouds (PSCs) and snow re-emission of nitrogen oxide species[Savarino et al., 2007]. N_2O oxidation, N_2 dissociation and photo-ionization establish the upper atmospheric sources [Brasseur and Solomon, 1986]. Less enrichment in LAX and Palmdale NO_3 is due to proximity to the source as the mixing occurs between primary

NO_3 particles emitted during combustion ($\Delta^{17}O=0$) and photochemically aged particles, thus lowering both $\delta^{18}O$ and $\delta^{17}O$ values. The average $\Delta^{17}O$ from Palmdale is 10.10 ‰ whereas the average $\Delta^{17}O$ from Palmdale and LAX is 17.31 and 40.40 ‰, respectively. Samples from La Jolla show higher $\Delta^{17}O$ than LAX and Palmdale serving as a remote background of NOx in an environment dominated by maritime air and fossil fuel burning (both of which are evolved NOx species). Due to proximity to the local ozone source (airplane emission), Palmdale's NO_3 data indicates that the oxygen isotopic anomaly increases with photochemical age and transport.

II. Los Angeles International Airport, Los Angeles, CA (33.9471°N, 118.4082°W, 38m)

Los Angeles International Airport (LAX) is the third busiest airport in the United States and sixth in the world with 600+ daily domestic flights and 1000+ weekly international flights on nearly 75 air carriers. ACI's 2010 report lists LAX as 13th in the world for air cargo tonnage processed [Airports Council International, 2010].

The results of isotopic measurements from three campaigns at LAX from October 2009 to March 2010 are shown in Figure 9. Best fit lines drawn through each seasonal campaign show an average slope of 0.40± 0.03 . The isotopic composition represents the steady state balance between tropospheric ozone and H_2O (intercept at $\delta^{18}O$= -5‰, $\Delta^{17}O$ = 0).

The seasonal variations are depicted with different y-intercepts (not through the origin) indicating mass independent fractionation and slight changes in reaction chemistry (Figure 9). If the line of best fit had a y-intercept of 0, this would imply mass dependent fractionation. However, the various y-intercepts were 4-6‰ different from the origin thereby implying mass independent fractionation occurred in the nitrate isotopes. As all seasons sampled do not have the same exact y-intercept but exhibit slight variability, a combination of mass dependent and mass independent fractionations in varying amounts may have occurred.

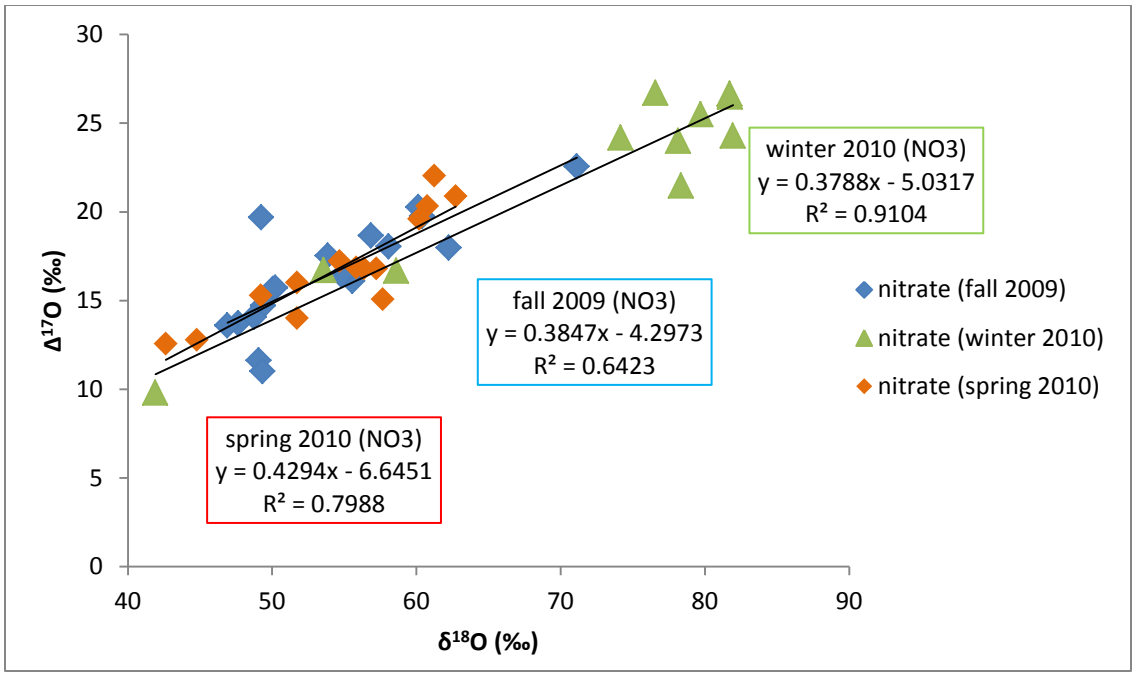

Figure 9: Seasonal representation of $\delta^{18}O$ and $\Delta^{17}O$ collected from LAX.

Global and regional production of HNO_3 models are consistent with observed LAX data implying a seasonal shift from homogeneous reactions in the spring to heterogeneous reaction in the winter [Dentener and Crutzen, 1993; Russell, McRae, and Cass, 1985; Michalski et al. 2003]. The observed maximum values of $\Delta^{17}O$ in the winter indicate dominance of the N_2O_5 hydrolysis reaction and no isotopic exchange during the hydrolysis reaction as complete isotopic exchange would remove the $\Delta^{17}O$ signal. The lifetime of the hydrolysis intermediate NO_2^+ is ~10s [Mendel and Wahner, 1999] before it is converted to HNO_3 which typically does not undergo isotopic exchange in the troposphere because the lifetime of the exchange is longer than the lifetime of nitrate [Bunton, Halevi and Llewellyn, 1952; Michaleski et al, 2003]. The contribution of the nitrate radical is small with maximum of 10‰ despite being an important nighttime sink for NMHC and DMS in the PMBL [Michalski et al., 2003].

Seasonal variation is not due to pressure and temperature effects [Morton et al, 1990]. Kendall and McDonnell (1998) suggests that the $\Delta^{17}O$ and $\delta^{18}O$ variability is due to different point sources of tropospheric water vapor of differing oxygen isotopic composition and the temperature dependence of kinetic fractionation factors in all reactions which vary with season and location [Kendall and McDonnell, 1998]. Michalski et al. 2003 suggests $\Delta^{17}O$ and $\delta^{18}O$ variability is due to differences in oxidative pathways that depend on the source conditions (ie plume vs dispersed background sources and varying contributions) [Michalski et al., 2003]. Consistent with previous studies, our data suggests aircraft emissions possess seasonal variability due to oxidative pathway, temperature and source (Figure 8).

Conclusions

The oxygen isotopic anomaly in nitrate emitted from aircraft fuels can serve as an important tracer of ozone interaction because oxygen triple isotope (^{16}O, ^{17}O, and ^{18}O) measurements have the potential to identify sources of oxygen atoms acquired during chemical transformation, resolve reaction mechanism and the extent of reaction. Using $\Delta^{17}O$, we have detected primary NO_3 being emitted from aircraft plumes which has a single oxygen isotopic composition and, appears to be the only nitrate source with this character. All other nitrate derives from evolution of NOx species with different fractionations depending upon chemistry and temperature. The ability to trace NOx oxidation pathways using $\Delta^{17}O$ of NO_3 offers new possibilities for studying the evolution of plume chemistry and effects on ozone. At present, there is no means by which aircraft emissions in a given region may be directly determined. Nitrate concentrations alone do not allow for assessment due to the issue of multiple sources. As a consequence, the impact of varying fuel type, and, increases in aviation traffic in the future in specific regions is difficult to determine. The isotopic measurements may add another means, independent of others, to make jet derived assessment possible, or improved.

Nitrate levels are the direct result of changes in NOx emissions and oxidation conditions that influence and reflect the physical and chemical properties of the atmosphere. NOx emissions are changing with decreasing concentrations in already industrialized countries due to improved technology and fuel changes whereas industrializing countries emit increasing quantities of NOx with intensified use of fossil

fuels. With these unpredictable changes in NOx emissions, new technologies will be developed.

Nitrogen isotopes ($^{15}N/^{14}N$ expressed as $\delta^{15}N$) could serve as a source signature. The oxygen isotopic measurements show that the isotopic character of molecular oxygen is preserved in the product nitrate because of the high temperature and pressure regime. These observations suggest that nitrogen may also have a value that is equal to that of molecular nitrogen. Essentially no, or few sources have this composition, thus nitrate would have both unique oxygen and nitrogen isotopic compositions, which further increases it ability to resolve sources in air. In the future, a combination of oxygen and nitrogen isotopes can be used a useful tool in providing parameters for atmospheric chemistry modeling in the photochemistry of NOx and to evaluate the sources.

This work was funded in part by the US Federal Aviation Administration Office of Environment and Energy under FAA Award Number: 07-C-NE-UMR, Amendment No. 008.

Chapter 3, in part is currently being prepared for submission for publication of the material. R. Shaheen, A. Hill, T. Jackson, S. Chakraborty, The thesis author was the primary investigator and author of this material.

Appendix:

Table 2: Palmdale Isotopic Measurements

sample	distance from jet (m)	fuel; air temp	Cl (mmol/m3)	NO3 (mmol/m3)	SO4 (mmol/m3)	$d^{18}O$ NO3 (‰)	$d^{17}O$ NO3 (‰)	$\Delta^{17}O$ NO3 (‰)	$d^{18}O$ SO4 (‰)	$d^{17}O$ SO4 (‰)	$\Delta^{17}O$ SO4 (‰)
090128-5a	1	FT1 hot	0.082	0.500	0.203	22.75	11.76	-0.07	31.00	16.12	0.00
090130-5a	1	FT2 hot	0.114	0.548	0.234	23.47	12.03	-0.18	28.13	14.61	-0.02
090202-5a	1	JP8 cold	0.049	0.169	0.377	26.69	13.66	-0.22	25.90	13.28	-0.19
090129-5a	3	"APU" hot	0.744	1.359	1.510	22.19	12.03	0.50	17.28	9.48	0.50
090126-Fbulka	30	JP8 hot	0.022	0.011	0.040	40.40	22.34	1.33	18.68	10.08	0.37
090127-5a	30	JP8 hot	0.027	0.025	0.071	38.48	24.01	4.00	16.37	8.56	0.05
090128-5a	30	FT1 hot	0.032	0.039	0.034	47.78	34.85	10.01	19.42	10.54	0.44
090130-5a	30	FT2 hot	0.000	0.000	0.000	33.82	22.65	5.07	17.03	9.08	0.23
090125-4	145	bgd; variable	0.000	0.000	0.000	70.44	63.04	26.41	6.94	5.18	1.57
090125-5b	145	bgd; variable	0.000	0.001	0.000	22.19	13.82	2.28	10.69	7.84	2.28
090128-5a	145	FT1 hot	0.021	0.013	0.008	54.92	46.09	17.53	19.67	16.01	5.79
090128-5b	145	FT1 hot	0.000	0.000	0.000	54.92	46.09	17.53	19.67	16.01	5.79
090130-5a+5b	145	FT2 hot				53.88	40.44	12.43	8.86	7.73	3.12
090131-5a+5b	145	FT2 cold				27.67	19.42	5.03	14.26	8.75	1.33
090131-5a+b	145	FT2+JP 8 hot				59.68	50.14	19.10	21.19	14.85	3.84

Table 3: LAX Fall 2009 Isotopic Measurements

sample	Cl (ppm)	SO4 (ppm)	NO3 (ppm)	$d^{18}O$ NO3 (‰)	$d^{17}O$ NO3 (‰)	$\Delta^{17}O$ NO3 (‰)	$d^{18}O$ SO4 (‰)	$d^{17}O$ SO4 (‰)	$\Delta^{17}O$ SO4 (‰)
LAX1-25R-6Oct09-5A	19.644	89.642	45.690	62.24	50.35	17.98	12.12	6.85	0.55
LAX2-PBSJ-6Oct09-5A	30.984	50.147	58.519	50.07	41.69	15.65	9.17	5.64	0.87
LAX3-LOTC-6Oct09-5A	31.454	62.111	58.430	60.13	51.54	20.27	7.88	5.17	1.08
LAX4-LOTB-DRK-6Oct09-5A	23.227	16.897	15.210	47.65	38.50	13.72	10.03	6.34	1.13
LAX1-25R-07Oct09-5A	20.030	18.381	6.922	49.06	37.15	11.64	13.62	8.15	1.07
LAX2-PBSJ-14Oct09-5A	8.194	74.588	24.198	46.91	38.00	13.61	11.08	6.91	0.77
LAX3-LOTC-14Oct09-5A	14.341	126.981	31.331	53.86	45.53	17.53	11.97	7.01	0.79
LAX4-LOTB-DRK-14Oct09-5A	10.188	45.827	16.740	55.58	45.01	16.11	11.05	6.58	0.83
LAX1-25R-19Oct09-5A	5.953	186.467	42.823	49.33	36.67	11.01	12.77	7.49	0.85
LAX2-PBSJ-19Oct09-5A	7.090	89.068	62.028	54.84	44.94	16.43	10.64	6.81	1.28
LAX3-LOTC-19Oct09-5A	12.003	174.241	105.309	49.39	40.40	14.72	12.96	7.82	1.08
LAX4-LOTB-19Oct09-5A	14.852	15.252	28.474	71.12	59.55	22.57	13.69	8.44	1.32
LAX1-25R-23Oct09-5A	14.17	83.684	65.956	50.22	41.85	15.73	14.76	8.36	0.69
LAX2-PBSJ-23Oct09-5A	14.26	38.625	58.736	48.76	39.44	14.09	9.69	6.41	1.37
LAX3-LOTC-23Oct09-5A	16.75	60.664	114.639	60.40	51.18	19.77	11.58	7.31	1.29
LAX4-LOTB-23Oct09-5A	15.93	45.081	64.838	56.85	48.24	18.67	11.89	7.59	1.41
LAX1-25R-23Oct09-1	127.12	41.932	34.339	58.08	48.25	18.05	10.56	6.20	0.71
LAX1-25R-23Oct09-2	137.07	69.984	121.597						
LAX1-25R-23Oct09-3	35.70	27.964	87.593						
LAX1-25R-23Oct09-4	18.89	26.800	77.241						
LAX4-LOTB-23Oct09-1	173.40	31.500	53.611	49.24	45.31	19.70	9.08	5.05	0.32
LAX4-LOTB-23Oct09-2	128.58	30.840	138.416						
LAX4-LOTB-23Oct09-3	35.64	19.342	95.859	53.97	45.42	17.36	12.71	7.15	0.54
LAX4-LOTB-23Oct09-4	18.30	27.731	73.908						
Fall Seasonal Average	39.80	62.00	61.24	54.09	44.68	16.56	11.43	6.91	0.94
Fall Stdev	48.23	46.39	35.20	6.26	5.95	3.01	1.79	0.98	0.31

Table 4: LAX Winter 2010 Isotopic Measurements

sample	Cl (ppm)	SO4 (ppm)	NO3 (ppm)	$d^{18}O$ NO3 (‰)	$d^{17}O$ NO3 (‰)	$\Delta^{17}O$ NO3 (‰)	$d^{18}O$ SO4 (‰)	$d^{17}O$ SO4 (‰)	$\Delta^{17}O$ SO4 (‰)
LAX1-25R-04Jan10-5A	10.00	77.75	54.41	41.91	31.61	9.81	16.60	9.00	0.37
LAX2-PBSJ-04Jan10-5A	14.71	14.55	43.46	53.56	44.57	16.71	12.74	8.03	1.41
LAX3-LOTC-04Jan10-5A	14.21	35.96	68.35	58.60	47.16	16.69	11.23	6.80	0.96
LAX4-LOTB-04Jan10-5A	13.03	25.97	68.34				9.01	5.84	1.15
LAX1-25R-07Jan10-5A	16.20	55.39	116.45	81.95	66.91	24.30	16.14	8.79	0.40
LAX2-PBSJ-07Jan10-5A	18.12	17.20	93.44	81.73	68.99	26.49	15.89	9.16	0.90
LAX3-LOTC-07Jan10-5A	20.99	32.35	186.51	76.58	66.53	26.71	16.51	9.46	0.87
LAX4-LOTB-07Jan10-5A	17.06	26.03	101.98	81.72	69.16	26.66	16.78	9.93	1.20
LAX1-25R-11Jan10-5A	11.40	77.16	78.91	74.16	62.74	24.18	18.33	9.88	0.35
LAX2-PBSJ-11Jan10-5A	16.03	24.50	73.25	79.70	66.95	25.51	13.27	8.06	1.16
LAX3-LOTC-11Jan10-5A	15.53	53.10	130.79	78.35	62.22	21.48	15.12	8.86	1.00
LAX4-LOTB-11Jan10-5A	14.76	39.66	86.89	78.16	64.64	24.00	17.19	9.59	0.66
LAX1-25R-14Jan10-5A	7.42	71.34	55.22				21.20	11.49	0.47
LAX2-PBSJ-14Jan10-5A	9.31	31.18	40.58	59.52	46.58	15.62	19.81	11.27	0.96
LAX3-LOTC-14Jan10-5A	9.81	54.94	142.51				18.68	10.59	0.88
LAX4-LOTB-14Jan10-5A	7.76	53.80	47.25	48.04	39.14	14.16	19.70	10.98	0.74
Winter Seasonal Average	13.99	42.40	90.34	68.77	56.71	20.95	16.28	9.32	0.85
winter stdev	3.91	20.66	40.57	14.35	12.98	5.65	3.27	1.55	0.32

Table 5: LAX Spring 2010 Isotopic Measurements

sample	Cl (ppm)	SO4 (ppm)	NO3 (ppm)	$d^{18}O$ NO3 (‰)	$d^{17}O$ NO3 (‰)	$\Delta^{17}O$ NO3 (‰)	$d^{18}O$ SO4 (‰)	$d^{17}O$ SO4 (‰)	$\Delta^{17}O$ SO4 (‰)
LAX1-25R-05Mar10-5A	15.39	64.65	27.30	57.68	45.07	15.08	17.60	9.44	0.29
LAX2-PBSJ-05Mar10-5A	24.37	11.58	19.58	60.21	50.91	19.60	10.50	6.60	1.14
LAX3-LOTC-05Mar10-5A	21.30	17.78	22.19				13.18	7.98	1.13
LAX4-LOTB-05Mar10-5A	21.67	21.16	36.12	60.75	51.92	20.33	12.74	7.44	0.81
LAX1-25R-09Mar10-5A	22.26	70.46	41.19	49.22	40.89	15.29	12.17	7.16	0.83
LAX2-PBSJ-09Mar10-5A	19.01	35.16	32.14	57.22	46.56	16.80	9.58	6.37	1.39
LAX3-LOTC-09Mar10-5A	20.43	35.73	35.77	51.74	40.92	14.02	13.04	7.77	0.99
LAX4-LOTB-09Mar10-5A	14.29	53.74	54.77	62.73	53.50	20.88	11.42	7.18	1.24
LAX1-25R-12Mar10-5A	27.64	65.66	46.24	55.83	45.89	16.85	17.08	10.51	1.63
LAX2-PBSJ-12Mar10-5A	24.87	29.49	37.68	51.74	42.92	16.02	14.18	11.16	3.79
LAX3-LOTC-12Mar10-5A	28.16	39.13	44.11	61.26	53.89	22.03	15.88	11.57	3.31
LAX4-LOTB-12Mar10-5A	22.58	43.59	44.94	54.68	45.65	17.22	14.89	11.57	3.83
LAX1-25R-16Mar10-5A	21.81	88.10	48.23	42.64	34.73	12.56	16.00	9.07	0.75
LAX2-PBSJ-16Mar10-5A	21.40	29.77	41.52	44.78	36.08	12.79	9.97	7.31	2.12
LAX3-LOTC-16Mar10-5A	22.97	39.35	57.37	56.38	46.12	16.81	8.58	6.20	1.74
Spring Seasonal Average	21.88	43.02	39.28	54.78	45.36	16.88	13.12	8.49	1.67
spring stdev	3.78	21.52	10.89	6.11	5.95	2.94	2.80	1.92	1.12

References:

Air Resources Board/Planning and Technical Support Division.
002. California Ambient Air Quality Data – 1980 – 2001.Sacramento, CA.: December 2005. Data CD Number: PTSD-02-017-CD

Airports Council International. Cargo Traffic 2010 Final Report. 2009.

Alexander, B., J. Savarino, K.J. Kreutz, and M.H. Thiemens (2004), Impact of preindustrial biomass- burning emissions on the oxidation pathways of tropospheric sulfur and nitrogen, J. Geophys. Res., 109, D08303, doi:10.1029/2003JD004218.

Baughcum, S.L., 1996. Subsonic aircraft emission inventories. In: Thompson, A.M., Friedel,R.R.,Wesoky, H.L. (Eds.), Atmospheric Effects of Aviation: First Report of the Subsonic Assessment Project. NASA Reference Publication 1385, Chapter 2.

Bisio, A. 1995. Aircraft Fuels. Encyclopedia of Energy, Technology and the Environment. New York, NY.

Bohlke, J.K., Mroczkowski, S. J., Coplen, T.B. 2003. Oxygen isotopes in nitrate: new reference materials for 18O:17O:16O measurements and observations on nitrate water equilibration. *Rapid Commun. Mass Spectrom*. 17, 1835-1846.

Brasseur, G. and Solomon, S. 1986. Aeronomy of the middle atmosphere, 452 pp., Reidel, D., Norwell, MA.

Brown, S.S., Ryerson, T.B., Wollny, A.G., Brock, C.A., Peltier, R., Sullivan, A.P., Weber, R.J., Dube, W.P., Trainer, M., Meagher, J.F.; Fehsenfeld, F.C.; Ravishankara, A.R.. Variability in Nocturnal Nitrogen Oxide Processing and Its Role in Regional Air Quality. Science 2006 volume 311 pg 67-70.

Finlayson-Pitts, B., and Pitts, J. Chemistry of the Upper and Lower Atmosphere: Theory, Experiments, and Applications. Academic Press: 2000.

Gaffney, J.S.; Marley, N.A. The impacts of combustion emissions on air quality and climate- from coal to biofuels and beyond. Atmospheric Environment 43 (2009) 23–36

Garcia-Naranjo, A., Wilson, C.W., 2005. Primary NO2 from Aircraft Engines Operating over the LTO Cycle. Report RC110187/05/01. Department of Mechanical Engineering, University of Sheffield, Sheffield, UK.

Hsiao-Hsien Hsu, Gary Adamkiewicz, E. Andres Houseman, Jose Vallarino, Steven J. Melly, Roger L. Wayson, John D. Spengler, Jonathan I. Levy. The relationship

between aviation activities and ultrafine particulate matter concentrations near a mid-sized airport. Atmospheric Environment, Volume 50, April 2012, Pages 328–337

IPCC (2007) 4th Assessment Report of the Intergovernment Panel on Climate Change. IPCC Geneva,Switzerland.

IPCC (1999) Aviation and the Global Atmosphere. IPCC Geneva, Switzerland.

Johnston, J.C.; Thiemens, M.H. The isotopic composition of tropospheric ozone in three environments, J. Geophys Res., 102 (D2) 25395-25404, 1997.

Kendall, C. and McDonnell, J.J. 1998. Isotope Tracers in catchment Hydrology. Elsevier, Amsterdam.

Kroopnick, P.; Craig, H. Atmospheric oxygen: isotopic composition and solubility fractionation. Science. 175 (4017), 54-55, 1972.

Laj, P., Klausen, J., Bilde, M., Pla-Duelmer, C., Pappalardo, G., Clerbaux, C., Baltensperger, U., et al. Measuring atmospheric composition change, Atmos. Environ., 43,5351-5414, 2009.

Lee, D.S., Fahey, D.W., Forster, P.N., Newton, P.J., Wit, R., Lim, L.L., Owen, B., Sausen, R. Aviation and global climate change in the 21st century, Atmospheric Environment (2009),doi:10.1016/j.atmosenv.2009.04.024

D.S. Lee, G. Pitari, V. Grewe, K. Gierens, J.E. Penner, A. Petzold, M.J. Prather, U. Schumann, A. Bais, T. Berntsen, D. Iachetti, L.L. Lim, R. Sausen. Transport impacts on atmosphere and climate: Aviation. Atmospheric Environment, Volume 44, Issue 37, December 2010, Pages 4678–4734

Lyons, J.R. (2001), Transfer of mass-indepenent fractionation on ozone to other oxygen-containing molecules in the atmosphere, Geophys. Res. Lett., 28, 3231-3234.

Mauersberger, K.; Lammerzahl, P., Krankowsky, D. Stratospheric Ozone Isotope Enrichments- revisited. Geophys res lett 28(16) 3155

Michalski, G., J.G. Bockheim, C.Kendall, and M. Thiemens, Isotopic composition of Antartic Dry Valley nitrate: Implications for NOy sources and cycling in Antartica, Geophyrical Research Letters, 32, 2005.

Michalski, G., Savarino, J. Bohlke, J.K., Thiemens, M.H. Determination of the total oxygen isotopic composition of nitrate and the calibration of a $\Delta^{17}O$ nitrate reference material. (2002) Anal. Chem. 74, 4989-4993.

Michalski, G., Scott, Z., Kabiling, M., Thiemens, M.H. First Measurements and modeling of $\Delta^{17}O$ in atmospheric nitrate. (2003) Geophys. Res. Lett., 30, 1870, doi:10.1029/2003GL017015

Michalski, G., J.G. Bockheim, C.Kendall, and M. Thiemens, Long term atmospheric deposition as the source of nitrate and other salts in the Atacama Desert, Chile: New evidence from mass-independent oxygen isotopic compositions, Geochimica et Cosmochimica Acta, 68, 4023-4038, 2004.

Miller, T.M., Ballenthin, J.O., Hunton, D.E., Viggiano, A.A., Wey, C.C., Anderson, B.E., 2003. Nitric acid emissions from the F100 jet engine. J. Geophys. Res. 108 (D1), 4032. doi:10.1029/2001JD001522.

Monks, P., Granier, C., Fuzzi, S., Stohl, A., Williams, M.L. Akimoto, H., Amann, M., Baklanov, A., Baltensperger, U., Bey, I., Blake, N., Carslaw, K., Cooper, O.R., Dentener, F., Fowler, D., Fragkou, E., Frost, G.J. et al.: Atmospheric composition change-global and regional air quality, Atmos. Environ., 43, 5268-5350, 2009.

Morin, S., R. Sander, and J. Savarino, Simulation of the diurnal variations of the oxygen isotope anomaly (Δ17O) of reactive atmospheric species, Atmos.Chem.Phys., 3653-3671,2011.

Savarino, J., Kaiser, J., Morin, S., Sigman, D. M., and Thiemens, M. H.: Nitrogen and oxygen isotopic constraints 1945, doi:10.5194/acp-7-1925-2007, 2007.

Sawyer, R.F., Harley, R.A., Cadle, S.H., Norbeck, J.M., Slott, R., Bravo, H.A., 2000. Mobile sources critical review: 1998 NARSTO assessment. Atmospheric Environment 34, 2161–2181.

Arnold, F., Scheid, J., Stilp, Th., Schlager, H., Reinhardt, M.E., 1992. Measurements of jet aircraft emissions at cruise altitude. 1. The odd-nitrogen gases NO, NO2, HNO2 and HNO3. Geophys. Res. Lett. 12 (24), 2421–2424.

Schulz, H. Short history and present trends of Fischer-Tropsch synthesis. Appl.Catal., A: 186 (1) 3-12.

Silva, S.R., Kendall, C., Wilkison, D.H., Ziegler, A.C., Chang, C.C.Y., Avanzino, R.J. A new method for collection of nitrate from fresh water and the analysis of nitrogen and oxygen isotope ratios (2000) J. Hydrol. 228, 22-36.

Tesseraux, I. (2004) Risk factors of jet fuel combustion products. Toxicology Letters. 149. Pages: 295-300.

Thiemens, M.H., Jackson, T., Zipf, E. C., Erdman, P.W. & van Egmond, C. Carbon dioxide and oxygen isotope anomaies in the mesosphere and stratosphere. Science 270 969-972.

Thiemens, M.H. 2006, History and Applications of Mass-Independent Isotope Effects. *Annu. Rev. Earth Plnet. Sci.* 34, 217-262.

Tremmel, H.G., Schalger, H., Konopka, P., Schulte, P., Arnold, F., Klemm, M., Droste- Franke, B., 1998.Observations and model calculations of jet aircraft exhaust products at cruise altitude and inferred initial OH emissions. J. Geophys. Res. 103 (D9), 10803–10816.

United States Government Accountability Office, Aircraft Emissions Expected to Grow, but Technological and Operational Improvements and Government Policies Can Help Control Emissions. Aviation and Climate Change report, June 2009.

Wagenbach, D., Legrand, M., Fischer, H., Pichlmayer, F. and Wolff, E. W. 1998. Atmospheric near-surface nitrate at coastal Antarctic sites. J. Geophys. Res., 103 (D9), 11 007-11 020.

Wormhoudt, J. S. Herdon, P. Yelvington, R. Miake-Lye. Nitrogen Oxide (NO/NO2/HONO) Emissions Measurements in Aircraft Exhausts. Journal of Propulsion and Power. Volume 23, No. 5, Sept-Oct 2007. Pages 906-911.